Effects of pressure on polaron energy shift in a wurtzite $Al_yGa_{1-y}N/Al_xGa_{1-x}N$ parabolic quantum well

FENG-QI ZHAO[a,*], ZI-ZHENG GUO[b,*]
[a]*College of Physics and Electronic Information, Inner Mongolia Normal University, Inner Mongolia Key Laboratory for Physics and Chemistry of Functional Materials,Hohhot 010022, People's Republic of China*
[b]*College of Electronic Engineering, South China Agricultural University, Guangzhou 510642, People's Republic of China*

The effect of hydrostatic pressure on the energy level of polaron and polaron energy shift in wurtzite $Al_yGa_{1-y}N/Al_xGa_{1-x}N$ parabolic quantum well (QW) is studied by a variational method. The numerical results of the ground state energy, transition energy and contributions of different phonons to polaron energy (polaron energy shift) are given as functions of pressure *p*, well width d, and composition *x*. In the theoretical calculation, the anisotropy of the parameters, such as the phonon frequency of different optical branches, the electron effective mass, the dielectric constant, etc., and their pressure and coordinate dependence are considered. The results show that the energy and transition energy of the polaron in the wurtzite $Al_yGa_{1-y}N/Al_xGa_{1-x}N$ parabolic QW decrease with the increasing of the hydrostatic pressure *p* and the well width *d*, and increase with the increasing of the composition *x*. The trends of the polaron energy shift with pressure *p*, well width *d* and composition *x* are obviously different. With the increase of hydrostatic pressure, the contribution of interface (IF) phonon slowly increases, while the contribution of confined (CF) phonon, half-space (HS) phonon and the total contribution of phonons of all branches increases obviously. During the increase of the well width, the contribution of CF phonon increases, and the contribution of HS phonon decreases, while the contribution of IF phonon and total contribution of phonons of all branches increase first and then decrease. With increasing the composition, the contribution of HS phonon decreases and the contribution of IF phonon increases slowly, while the contribution of CF phonon and the total contribution of phonons of all branches phonon increase significantly. The dependences of hydrostatic pressure, well width ,and composition *x* of the ground state energy, transition energy, and polaron energy shift of the polaron in the wurtzite $Al_yGa_{1-y}N/Al_xGa_{1-x}N$ parabolic QW structure are basically similar to that of the square $GaN/Al_xGa_{1-x}N$ QW structure, but the amplitude is different.

(Received March 15, 2019; accepted August 18, 2020)

Keywords: Wurtzite parabolic quantum well, Hydrostatic pressure, Polaron, Polaron energy shift

1. Introduction

The wurtzite nitride semiconductors of group-III with wide-band-gap and related compound materials have attracted much attention due to their significant potentials for electronic and optical applications [1-5]. Until now, GaN-based quantum well (QW) materials have been applied in laser diodes, light emitting diodes, phototubes, ultraviolet photodetectors and other devices [6-15]. The earlier successful work on polaron properties in III-V wurtzite nitride compounds and heterostructures can be traced back to the calculations of M.E. Mora‐Ramos et al. ,in which the uniaxial dielectric continuum model were used[16-21]. Lee et al.[22] and Shi et al.[23,24] derived the Frohlich Hamiltonian for the electron-optical phonon interactions (EOPI) in the wurtzite heterojunction and QW structure by using the continuous medium and transfer matrix method, respectively. Their results indicate that, in the single wurtzite QW structure, there are four long-wave optical phonon modes with electronic interactions. These include a confined (CF) phonon mode, half space (HS) phonon mode, interface (IF) phonon mode, and propagating (PR) phonon mode.

The linear and nonlinear intraband optical absorptions in semi-parabolic QWs [25-29] were theoretically investigated in detail by using different methods. The effects of electric and magnetic fields on the linear and nonlinear optical properties of the semi-parabolic QWs were studied using the effective-mass approximation and the compact density-matrix approach [30-38]. The changes in the refractive index and intraband optical absorption coefficients in symmetric double semi-V-shaped QWs were investigated theoretically within the effective-mass approximation framework [39]. The effects of the structure parameters such as the right-well width and the right-barrier height on the linear, third-order nonlinear and total absorption and refractive index changes of asymmetric double semi-V-shaped quantum well were theoretically studied by using the compact-density matrix approach and iterative method [40]. The linear and the third-order nonlinear optical absorptions in the asymmetric double triangular QWs were investigated theoretically by using the compact density-matrix approach and the iterative method [41]. The effect of the electron‐phonon interaction（EPI） on the optical rectification was investigated theoretically for electrons confined in semi-parabolic QWs [42]. In our previous work, with the help of the Frohlich Hamiltonian derived by Liang et al.[43] and Lee et al.[22], the polaron energy and transition energy as well as the energy shift caused by the EOPIs in zinic-blende $Al_yGa_{1-y}As/Al_{0.3}Ga_{0.7}As$ [44-46] and wurtzite nitride [47] parabolic QW materials have been discussed.

The hydrostatic pressure modification of the physical properties of nitride based low-dimensional structures is

available and helpful for exploring new phenomena and improving devices [48]. Pressure can effectively shorten the distance between the atoms of the material and increase the overlapping of adjacent electron orbits, thereby changing the crystal structure, the electronic structure and the interaction between the atoms (molecules) to form a new material state. These kinds of new material state are hard to exist under normal pressure and have different atmospheric structure, novel physical and chemical properties. The hydrostatic pressure behavior of material physical parameters, such as energy gaps, the effective masses, phonon frequencies, dielectric constant were investigated in the Refs.49-52 The intraband transitions in square and parabolic QWs under simultaneous action of the hydrostatic pressure and high-frequency laser field have been investigated [53]. They found that the laser-induced blue shift effect on the subband energy levels may be tuned by the pressure action. However, there are few reports currently available regarding the influences of hydrostatic pressure on the polaron energy level and polaron energy shift in wurtzite $Al_yGa_{1-y}N/Al_xGa_{1-x}N$ parabolic QW materials.

In this paper, a variational method is used to study the effects of hydrostatic pressure on the polaron energy level and polaron energy shift in $Al_yGa_{1-y}N/Al_xGa_{1-x}N$ parabolic QW structures. The functions of polaron energy, transition energy, and polaron energy shift as hydrostatic pressure *p*, the well-width *d* and composition *x* are given. The theoretical calculations take into account the anisotropies of the optical phonon frequency, dielectric constant, electron effective mass, and other parameters of the system, as well as their change factors with pressure *p* and coordinate *z*.

2. Model and theoretical derivation

A wurtzite $Al_yGa_{1-y}N/Al_xGa_{1-x}N$ parabolic QW is composed of multi-layer materials, with the well-material $Al_yGa_{1-y}N$ a continuous composition *y* setting from zero to *x*. The barrier material $Al_xGa_{1-x}N$ is located in the interval of $|z| > d/2$ with *d* the well width. The parameters of the phonon frequency, dielectric constant, and electronic effective mass in the well-materials change continuously with coordinate *z*. The composition *y* and coordinate *z* display the relationship of $y = 4xz^2/d^2$, in contrast to the $GaN/Al_xGa_{1-x}N$ square QW structure, where the parameters of the well-material (GaN) are constant. The coordinate X-Y plane is parallel to the QW interface, and the axis Z is selected as being perpendicular to the QW interface. By utilizing an effective mass approximation, and considering the anisotropy of the wurtzite structure, the Hamiltonian of the free polaron system can be written as follows:

$$H = p_z\left(\frac{p_z}{2m_{z\lambda}}\right) + \frac{p_\perp^2}{2m_{\perp\lambda}} + V(z) + \sum_{\vec{w}j} \hbar\omega a_j^+(\vec{w}) a_j(\vec{w}) + H_I \qquad (1)$$

where $m_{\perp\lambda}$ and $m_{z\lambda}$ represent the electron effective mass of material (λ = 1 for the well material, λ =2 for the barrier material); $a_j(\vec{w})$ and $a_j^+(\vec{w})$ are the annihilation operator and creation operator with frequency ω and wave vector $\vec{w}$ ($\vec{w} = (\vec{q}, k_{\lambda z})$ for CF and HS phonons, and $\vec{w} = \vec{q}$ for IF phonons), respectively; $j = \{s, r\}$, in which *s* represents the symmetric and antisymmetric phonon mode, and *r* represents CF, HS and IF phonon modes (including the longitudinal optical (LO) and transverse optical (TO) phonons), respectively; and $V(z)$ is a potential function written as follows:

$$V(z) = \begin{cases} 4V_0 z^2/d^2, & |z| < d/2, \\ V_0, & |z| \geq d/2, \end{cases} \qquad (2)$$

where,

$$\begin{aligned} V_0 &= 0.7\Delta E_g = E_g(Al_xGa_{1-x}N) - E_g(GaN) \\ &= x[E_g(AlN) - E_g(GaN)] + bx(x-1) \end{aligned} \qquad (3)$$

$E_g(GaN)$, $E_g(AlN)$, $E_g(Al_xGa_{1-x}N)$ are the band gap of alloy GaN, AlN and $Al_xGa_{1-x}N$, the adjustment parameter *b* is taken as 1.0 eV [54], and *e* is the basic charge. The Hamiltonian with the EOPI can be expressed as follows:

$$H_I = \sum_{\vec{w}j} [g_j(z) \exp(i\vec{q}\cdot\vec{\rho}) a_n(\vec{w}) + h.c], \qquad (4)$$

where $\vec{q}$ and $\vec{\rho}$ are phonon wave vector and electron position vector on plane X-Y, respectively. For the symmetric CF phonons, the coupling function can be expressed as follows [22]:

$$g_{S,CF} = -i\left[\frac{4\pi\hbar e^2 L^{-2}}{(\partial/\partial\omega)(\varepsilon_{1\perp}q^2 + \varepsilon_{1z}k_{1m}^2)d/2 - 2q(\partial/\partial\omega) f_s(\omega)\cos(k_{1m}d/2)}\right]^{1/2} \times \chi_{S,CF}, \qquad (5)$$

where

$$\chi_{S,CF} = \begin{cases} \cos(k_{1m}z), & (|z| < d/2) \\ \cos(k_{1m}d/2)\exp(-\kappa_2(|z| - d/2)), & (|z| \geq d/2) \end{cases}, \qquad (6)$$

$$\begin{aligned} f_s(\omega) = {} & \mathrm{sgn}(\varepsilon_{1z})\sqrt{-\varepsilon_{1\perp}(\omega)\varepsilon_{1z}(\omega)}\sin(k_{1m}d/2) \\ & -\mathrm{sgn}(\varepsilon_{2z})\sqrt{\varepsilon_{2\perp}(\omega)\varepsilon_{2z}(\omega)}\cos(k_{1m}d/2) \end{aligned},$$

in equation (5),

k_{1m} is determined by the equation $\varepsilon_{1z}k_{1m}\sin(k_{1m}d)-\varepsilon_{2z}k_2\cos(k_{1m}d)=0$, satisfying $2m\pi/d<k_{1m}<2(m+1)\pi/d$, m is the sum of a series of CF modes, and L^2 is the area of the QW interface. The direction-dependent dielectric functions $\varepsilon_{\lambda\perp}(\omega)$ and $\varepsilon_{\lambda z}(\omega)$, are given by:

$$\begin{cases}\varepsilon_{\lambda\perp}(\omega)=\varepsilon_{\lambda\perp}^{\infty}\dfrac{\omega^2-\omega_{\lambda\perp L}^2}{\omega^2-\omega_{\lambda\perp T}^2},\\ \varepsilon_{\lambda z}(\omega)=\varepsilon_{\lambda z}^{\infty}\dfrac{\omega^2-\omega_{\lambda\perp zL}^2}{\omega^2-\omega_{\lambda zT}^2},\end{cases} \tag{7}$$

where $\varepsilon_{\lambda\perp}^{\infty},\varepsilon_{\lambda z}^{\infty}$, $\omega_{\lambda\perp L},\omega_{\lambda zL},\omega_{\lambda\perp T},\omega_{\lambda zT}$ are the high frequency dielectric constant, LO, and TO optical phonon dispersion frequency vertical and parallel to the direction of the QW interface, respectively. A linear interpolation method was used to obtain the dielectric constant, phonon frequency, and electron effective mass of the ternary mixed crystal $Al_xGa_{1-x}N$（$Al_yGa_{1-y}N$）material, based on the corresponding parameters of the binary crystal AlN and GaN. For example: $Q_{Al_xGa_{1-x}N}=xQ_{AlN}+(1-x)Q_{GaN}$.

Similar to the symmetrical CF phonon, the coupling functions of the antisymmetric CF phonon, HS and IF phonon are detailed in reference [22]. The eigenfrequencies ω of the CF and HS phonon are determined with the related material parameters by using the equation $\varepsilon_{\lambda\perp}\sin^2\theta_\lambda+\varepsilon_{\lambda z}\cos^2\theta_\lambda=0$, and θ_λ is the angle between the wave vector $\overset{\vee}{w}$ and axis *Z*. The details for calculating the IF phonon eigenfrequencies can be found in reference [22].

The phonon frequency, electron effective mass, dielectric constant, band gap and other parameters are functions of hydrostatic pressure. The relationship between the band gap and hydrostatic pressure is [49]

$$E_{g\lambda}(p)=E_{g\lambda}+\alpha_\lambda p \tag{8}$$

in which $E_{g\lambda}$ is the band gap of the material at p=0, α_λ is the pressure coefficient. The relationship between the effective electron mass and the pressure is [50]

$$m_{\lambda a}(p)=\frac{m_{\lambda a}(E_{g\lambda}+\alpha_\lambda p)}{E_{g\lambda}+m_{\lambda a}\alpha_\lambda p} \tag{9}$$

where $a=\perp,z$ represent the direction perpendicular to the Z-axis direction and parallel to the Z-axis direction, respectively. The phonon frequency $\omega_{\lambda ab}$ changes with pressure as follows [48,51]

$$\gamma_{\lambda ab}=\frac{B_{0\lambda}}{\omega_{\lambda ab}}\frac{\partial\omega_{\lambda ab}(p)}{\partial p} \tag{10}$$

in which $\gamma_{\lambda ab}$ is a parameter, $B_{0\lambda}$ is the body modulus, $b=T,L$ stand for the TO and LO optical phonon. The high-frequency dielectric constant changes with pressure with the relationship [48,52]

$$\frac{\partial\varepsilon_{\lambda a}^{\infty}(p)}{\partial p}=\frac{5(\varepsilon_{\lambda a}^{\infty}-1)(f_{\lambda ion}-0.9)}{3B_{0\lambda}} \tag{11}$$

where $f_{\lambda ion}$ is the ionicity of the material under pressure.

The solving process can be simplified by means of twice unitary transformations on the Hamiltonian operator of the system. The unitary transformation form is set as follows:

$$\begin{cases}U_1=\exp[-i(\sum_{wj}\overset{\vee}{q}\cdot\overset{\vee}{\rho}a_j^{+}(\overset{\vee}{w})a_j(\overset{\vee}{w})],\\ U_2=\exp\{\sum_{\overset{\vee}{w}j}[\beta_j\chi_j a_j^{+}(\overset{\vee}{w})-\beta_j^{*}\chi_j a_j(\overset{\vee}{w})]\},\end{cases} \tag{12}$$

where β_j and β_j^{*} are the variational parameters determined by solving the system's energy minimum. The transformed Hamiltonian is as follows:

$$H^{*}=U_2^{-1}U_1^{-1}HU_1U_2 \tag{13}$$

The ground state wave function of the system is selected as follows:

$$\psi=C\varphi(z)\left|0\right\rangle \tag{14}$$

where $\left|0\right\rangle$ is the phonon vacuum state, and *C* is the normalized constant. The polaron energy E_n and the wave function $\varphi(z)$ of the electron along *Z* direction are determined by solving the Schrodinger equation numerically. The transition energy from the ground state to the first excited state can be given by

$$\Delta E=E_1-E_0 \tag{15}$$

For comparison we also calculated the energy of a polaron in a square $GaN/Al_xGa_{1-x}N$ QW structure. The energies of the polaron in a square $GaN/Al_xGa_{1-x}N$ QW are obtained by a method similar to that for the parabolic QWs.

3. Numerical results and discussion

The polaron energy, as well as the contributions of the different phonon modes to energy, as the functions of the QW width *d*, hydrostatic pressure *p* and composition *x*, were obtained through the numerical calculation of the Schrodinger equation. The results are shown in Figs. 1 to 6. Also, the parameters used in the numerical calculation are listed in Table 1.

Table 1. The parameters for wurtzite QWs used in the calculation. The electron effective masses, phonon frequency, bulk modulus, and the band gap are in unit of electron rest mass m_e, meV, GPa,and eV, respectively

Materials	$m_\perp$	m_z	$\varepsilon_\perp^\infty=\varepsilon_z^\infty$	$\omega_{\perp T}$	ω_{zT}	$\omega_{\perp L}$	ω_{zL}	$\gamma_{\perp T}$	γ_{zL}	$\gamma_{\perp L}$	γ_{zL}	f_{ion}	B_0	E_g	α
GaN	0.19[55]	0.23[55]	5.7[56]	69.56[57]	66.08[57]	92.12[57]	91.13[57]	1.19[51]	1.21[51]	0.99[51]	0.98[51]	0.5[48]	207[58]	3.5[59]	3.3[60]
AlN	0.30[61]	0.32[61]	4.68[62]	83.44[62]	81.83[62]	113.57[62]	110.72[62]	1.18[51]	1.02[51]	0.91[51]	0.82[51]	0.499[48]	210[58]	6.28[59]	4.3[60]

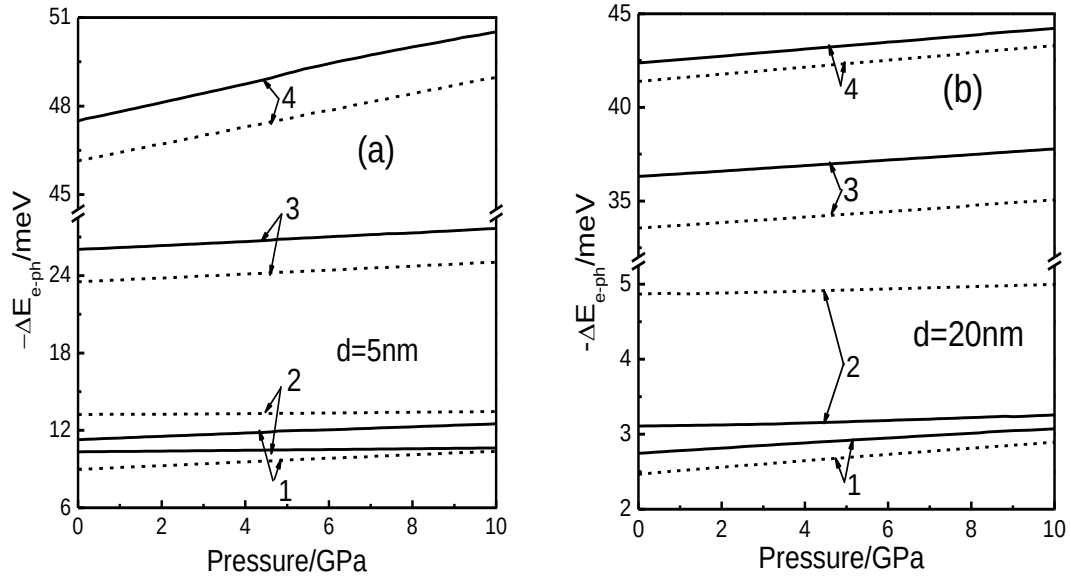

Fig. 1. Pressure dependence of the contributions of the EOPI to the polaron energy in the wurtzite $Al_yGa_{1-y}N/Al_{0.3}Ga_{0.7}N$ parabolic QW and $GaN/Al_{0.3}Ga_{0.7}N$ square QW for a given well width d. In Fig. 1(a), (b), the HS, IF and CF phonon contribution, as well as their sum, are indicated by Line 1, Line 2, Line 3 and Line 4, respectively. The results of the parabolic QW and square QW are indicated by the solid and dotted lines, respectively

Fig. 1 (a) and (b) show the pressure dependence of the contributions of the EOPI to the polaron energy in the wurtzite $Al_yGa_{1-y}N/Al_{0.3}Ga_{0.7}N$ parabolic QW and $GaN/Al_{0.3}Ga_{0.7}N$ square QW for a given well width *d*. As can be seen from Fig.1 that, for the cases *d*= 5 nm and *d*=20 nm, as the pressure increases from 0 GPa to 10GPa, the contribution of the IF phonons increases slowly with the increase of pressure *p*, which is 2.9% in the $Al_yGa_{1-y}N/Al_{0.3}Ga_{0.7}N$ parabolic QW (1.7% in the $GaN/Al_{0.3}Ga_{0.7}N$ square QW) and 4.8% (2.5%), respectively. The contributions of the HS,CF phonon and the total phonon increased obviously as pressure *p* increased with increasing rate of 10.9% (15.7%), 6.3% (6.5%), 6.4% (6.1%) for the case *d*=5nm, and 12.0% (17.2%),4.1% (4.5%), 4.4% (4.6%) for the case *d*=20nm. Fig. 1 shows that hydrostatic pressure increases the polaron energy shift. This can also be seen from equations (7) - (10): as the pressure *p* increases, the electron effective mass and the phonon frequency increase while the dielectric constant decreases. As well known that, the increase of the effective electron mass and the phonon frequency, and the decrease of the dielectric constant will lead to the increase of polaron energy shift in the QW. Fig. 1 also shows that the hydrostatic pressure dependence of the contribution of phonons of CF, HS and IF in parabolic QW structures and the contribution of total phonon contribution are basically similar to that of the square QW structures, but the amplitude is different.

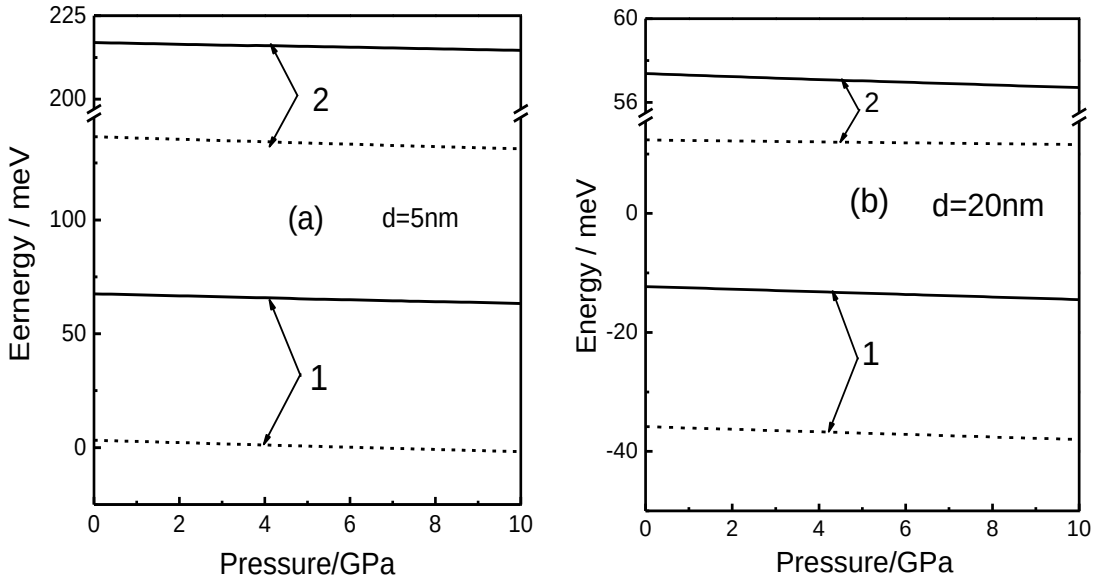

Fig. 2. Pressure dependence of polaron ground state energy and the transition energy in the $Al_yGa_{1-y}N/Al_{0.3}Ga_{0.7}N$ parabolic QW and $GaN/Al_{0.3}Ga_{0.7}N$ square QW for a given well width d. In Fig. 2 (a), (b), line 1 and line 2 represent the ground state energy and the transition energy, respectively. The solid and dotted lines represent the results of the parabolic QW and square QW, respectively

Fig. 2 depicts the pressure dependence of free polaron ground state energy (E_0) and the transition energy($\Delta E = E_1 - E_0$) in the $Al_yGa_{1-y}N/Al_{0.3}Ga_{0.7}N$ parabolic QW and $GaN/Al_{0.3}Ga_{0.7}N$ square QW for a given well width d. It can be seen from Fig. 2 (a) and (b) that both the E_0 and ΔE decrease slowly with the increasing of pressure. For the cases of d= 5 nm and d=20 nm, as the pressure increases from 0 GPa to 10GPa, the decrease of ΔE in the $Al_yGa_{1-y}N/Al_{0.3}Ga_{0.7}N$ parabolic QW ($GaN/Al_{0.3}Ga_{0.7}N$ square QW) reaches up to 1.1% (3.9%) and 1.2% (6.2%), respectively. Since the increasing of the hydrostatic pressure p can result in the increase of the electron effective mass and the polaron energy shift in the QW structure as explained in Fig. 1, it will naturally cause the ground state energy and the transition energy of the polaron to become smaller.

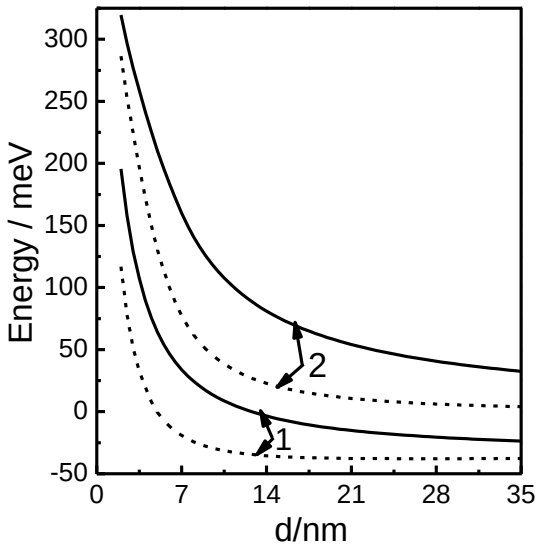

Fig. 3. Well width dependence of polaron ground state energy and the transition energy in the $Al_yGa_{1-y}N/Al_{0.3}Ga_{0.7}N$ parabolic QW and $GaN/Al_{0.3}Ga_{0.7}N$ square QW for a given pressure (p=8GPa). Line 1 and line 2 represent the ground state energy and the transition energy, respectively. The solid and dotted lines represent the results of the parabolic QW and square QW, respectively

The well width dependence of polaron ground state energy E_0 and the transition energy ΔE in the $Al_yGa_{1-y}N/Al_{0.3}Ga_{0.7}N$ parabolic QW and $GaN/Al_{0.3}Ga_{0.7}N$ square QW for a given pressure p is shown in Fig. 3. It can be seen from Fig. 3 that both E_0 and ΔE decrease with the increase of d, and they decrease faster when the well width d is smaller, and decrease more slowly when the well

width d is larger. These changes are the result of quantum confinement of electron in the QW structure. In narrow wells, the quantum confinement effect is strong, causing greater energy and transition energy. The case of wide wells is just the opposite. Fig. 3 also shows that the well width dependences of E_0 and ΔE in the $Al_yGa_{1-y}N/Al_{0.3}Ga_{0.7}N$ parabolic QW are basically the same with that in the $GaN/Al_{0.3}Ga_{0.7}N$ square QW, but in the former E_0 and ΔE are significantly greater. This is because the electron effective mass, dielectric constant and other parameters of the well material in the parabolic QW structure are changed continuously with z, which leads to the stronger quantum confinement effect in the parabolic QW compared with the square QW.

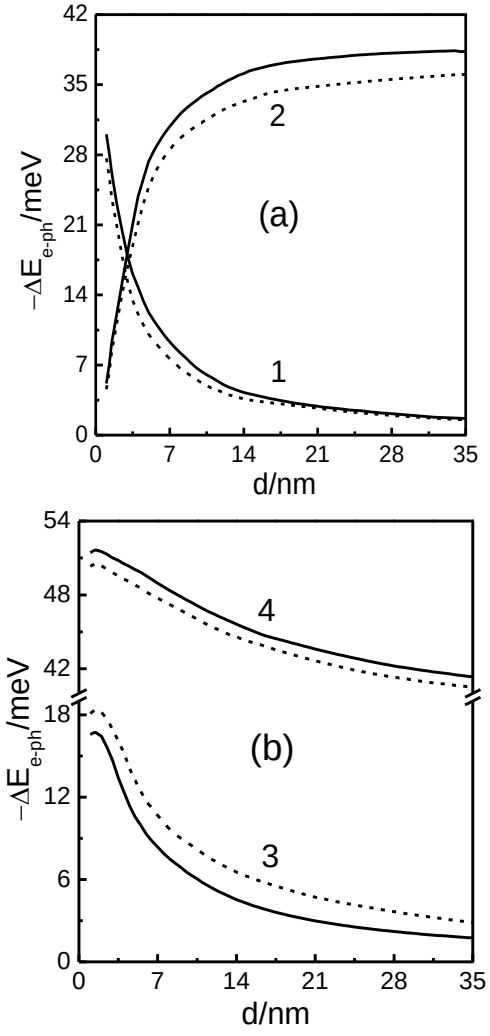

Fig. 4. Well width dependence of the contributions of the EOPI to the polaron energy in the wurtzite $Al_yGa_{1-y}N/Al_{0.3}Ga_{0.7}N$ parabolic QW and $GaN/Al_{0.3}Ga_{0.7}N$ square QW for a given pressure (p=8GPa). The HS,CF and IF phonon contribution, as well as their sum, are indicated by Line 1, Line 2, Line 3 and Line 4, respectively. The results of the parabolic QW and square QW are indicated by the solid and dotted lines, respectively

The well width dependence of the HS,CF and IF phonon contributions to the polaron energy (polaron energy shift) are also calculated for a given pressure p=8GPa (see Fig 4). It is shown that the contributions of different phonons to ground state energy are not the same, and the well width dependence trend is also different obviously. With the increase of the well width d , the contribution of the HS phonon decreases obviously, and the contribution of the CF phonon increases obviously . The IF phonon contribution and the total phonon contribution (the sum of the contributions of the three branch phonons) decrease with the increase of the well width d and in the decreasing process, the extreme value appears. The above phenomenon can be explained by the theory of electron tunneling. With the increase of d, the probability of electron penetrating into the barrier material becomes smaller and the wave function localization increases, in this way, the degree of coupling between electron and different branch phonons changes naturally. Figure 4 (a) and (b) also show that the contribution of IF phonon in the parabolic QW structure is smaller than that in the square QW structure, while the CF, HS phonon contributions as well as the total phonon contribution are larger than those in QW structure. Considering the differences of the structures of the two kinds of wells and differences of material parameters, such as the dielectric constant, the phonon frequency and the electron effective mass, we can understand these results easily.

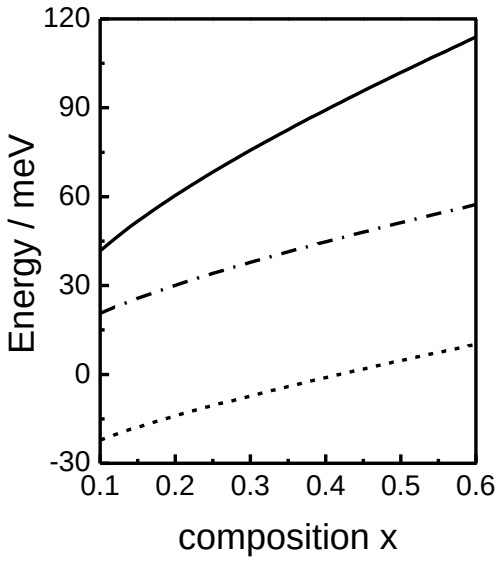

Fig. 5. Composition x dependence of polaron ground state energy and the transition energy in the wurtzite $Al_yGa_{1-y}N/Al_xGa_{1-x}N$ parabolic QW for a given well width (d=15nm) and pressure (p=8Gpa). The dotted, dashed dotted and solid lines indicate the results of the ground state energy (with EOPI), the ground state energy (without EOPI), and the transition energy (with EOPI), respectively

In Fig. 5, we plot the composition x dependence of polaron ground state energy and the transition energy in the wurtzite $Al_yGa_{1-y}N/Al_xGa_{1-x}N$ parabolic QW. We can know that in a parabolic QW with a fixed well width (here d=15nm) and pressure (here p=8GPa), E_0 increases slowly, and ΔE increases rapidly as x is increased. The reason for this phenomenon is that, as x increases, the potential barrier of the QW structure becomes higher, so that the confinement effect of the QW structure on the electron is enhanced, which leads to the increase of E_0 and ΔE .

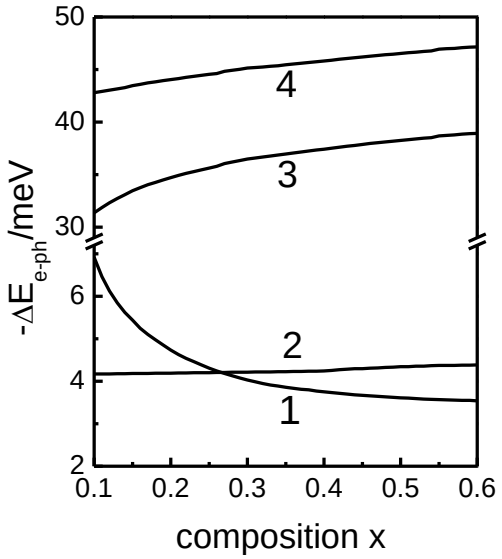

Fig. 6. Composition x dependence of the contribution of the different phonons to the polaron ground state energy in the $Al_yGa_{1-y}N/Al_xGa_{1-x}N$ parabolic QW for a given well width (d=15nm) and pressure (p=8GPa). Line 1,2 and 3 indicate the HS,IF and CF phonon contributions, respectively, and line 4 is the total phonon contribution

In Fig. 6, our calculation results reveal the composition x dependence of the contribution of the different phonons to the polaron ground state energy in the $Al_yGa_{1-y}N/Al_xGa_{1-x}N$ parabolic QW for a given well width (d=15nm) and pressure (p=8GPa). As can be seen from Fig. 6, with increasing x, the contribution of HS phonon decreases obviously, the contribution of IF phonon increases slowly, and the contribution of CF phonon and the total contribution of phonon increase significantly. In details, as composition x increases from 0.1 to 0.6, the contribution of HS phonon decreases by 48.8%, while the phonon contribution of IF and CF increases by 5.2% and 24.2%, respectively. This trend is mainly due to the fact that, as the composition x increases, the barrier of the QW becomes higher and the probability of electrons penetrating into the barrier material becomes smaller, which leads to different EPI situations: the coupling between electrons and HS phonons is weakened and the coupling between electrons and CF phonon is enhanced ,while the coupling between electron and IF phonon is not significantly changed, so the total phonon contribution slowly increases with the increase of composition x, up to 10.2%.

In the above calculation, we always assume that the energy band structure of AlGaN is a direct band gap. The literature indicates that the direct -indirect band gap transition does not occur in AlGaN over a pressure range from 0 GPa to 10 GPa [63].

4. Conclusions

By using the Lee-Low-Pines variational method, the pressure effects on polarons in the wurtzite $Al_yGa_{1-y}N/Al_xGa_{1-x}N$ parabolic QW structure and the square $GaN/Al_xGa_{1-x}N$ QW structure were investigated theoretically. The ground state energy, transition energy, and polaron energy shift caused by the EOPI were calculated numerically as the functions of hydrostatic pressure p, the well-width d and composition x . The anisotropy of the parameters in the system, such as the optical phonon frequency, dielectric constant, and electron effective mass, as well as their changes with pressure p and coordinate z were taken into account in the calculations. The results show that hydrostatic pressure affects the ground state energy, transition energy of the polaron and polaron energy shift in both wurtzite $Al_yGa_{1-y}N/Al_xGa_{1-x}N$ parabolic and $GaN/Al_xGa_{1-x}N$ square QWs. With the increase of pressure p, the ground state energy and transition energy of the polaron slowly decrease in both wells, and the contribution of different phonons to polaron energy increases, that is, the polaron effect increases significantly. Given composition x and hydrostatic pressure p, the ground state energy and transition energy of the polaron decrease with the increase of the well width d, and finally approach the corresponding value of the well material. The well width d dependences of contributions of different phonons to polaron energy behave differently. The contribution of CF phonon increases with the increase of well width. The contribution of HS phonon decreases with the increase of well width, while the contribution of IF phonon and the total contributions of phonons increase first and then decrease with the increase of well width. With the increase of composition x, the contribution of HS phonon decreases, the contribution of IF increases slowly and the contribution of CF phonon and the total contribution of phonons increase significantly for given well width d and hydrostatic pressure p. The dependences of hydrostatic pressure p, well width d, and composition x of the ground state energy, transition energy of the polaron, and polaron energy shift in the wurtzite $Al_yGa_{1-y}N/Al_xGa_{1-x}N$ parabolic QW structure are basically similar to that of the square $GaN/Al_xGa_{1-x}N$ QW structure, but the amplitude is different. Compared with the $Al_yGa_{1-y}As/Al_xGa_{1-x}As$ zinc-blende parabolic QW, in which the contribution of the

EOPI is smaller (1.8meV ~ 7.6meV) [44,46,64] , the contribution of the EOPI is larger (41meV ~ 52meV) in the wurtzite $Al_yGa_{1-y}N/Al_xGa_{1-x}As$ parabolic QW. Therefore, polaron effect should be considered in the study of the electron energy level in wurtzite $Al_yGa_{1-y}N/Al_xGa_{1-x}N$ parabolic QW materials. Our work in this research is very helpful to further study of the nano semiconductor low-dimensional structures with strong EOPIs.

Acknowledgments

This work is funded by the National Natural Science Foundation of China (Grant No. 11664031), the Natural Science Foundation of Inner Mongolia of China (Grant No. 2015MS0126), the project of Prairie Excellent Specialist of Inner Mongolia.

References

[1] S. Nakamura, Solid State Communications **102,** 237 (1997).
[2] W. Shan, W. Walukiewicz, K. M. Yu, J. W. Ager, E. E. Haller, J. F. Geisz, D. J. Friedman, J. M. Olson, Sarah R. Kurtz, C. Nauka, Physical Review B **62**, 4211 (2000).
[3] K.Nomura , H. Ohta, K. Ueda, T. Kamiya, M. Hirano, H. Hosono, Science **300,** 1269 (2003).
[4] U.Ozgur , Y. I. Alivov, C. Liu, A. Teke, A., M. A. Reshchikov, S. Doğan, V. Avrutin, S. J. Cho, H. Morkoc, Journal of Applied Physics **98,** 041301(2005).
[5] K. Akita, T. Kyono, Y. Yoshizumi, H. Kitabayashi, K. Katayama, Journal of Applied Physics **101,** 033104 (2007).
[6] F. A. Ponce, D. P.Bour, Nature **386,** 351 (1997).
[7] J. J.Wierer Jr., A. J. Fischer, D. D. Koleske, Applied Physics Letters **96,** 051107 (2010).
[8] W. Lee, M. H. Kim, D. Zhu, Journal of Applied Physics **107,** 063102 (2010).
[9] V. K. Malyutenko, S. S. Bolgov, A. D. Podoltsev, Applied Physics Letters **97,** 251110 (2010).
[10] H. P. Zhao, G. Y. Liu, R. A. Arif, N.Tansu, Solid State Electronics **54**,1119 (2010).
[11] O. Joachim Piprek, Applied Physics Letters **109,** 021104 (2016).
[12] Z. H. Zhang, Y. H. Zhang, W. G. Bi, C. Geng, S. Xu, H. V. Demir, X. W. Sun, Applied Physics Letters **108,** 151105 (2016).
[13] X. Y. Yi, H. Q. Sun, J. Sun, Yang, X. C. Fan, Z. D. Zhang, Z. Y. Guo, Superlattices and Microstructures **104,** 19 (2017).
[14] L. Lu, Z. Wan, F. J. Xu, X. Q.Wang, C. Lv, B. Shen, M. Jiang, Q. G. Chen, Superlattices and Microstructures **104,** 240 (2017).
[15] H. Condori Quispe, S. M. Islam, S. Bader, A. Chanana, K. Lee, R. Chaudhuri, A. Nahata, H. G. Xing, D. Jena, B. Sensale-Rodriguez, Applied Physics Letters **111,** 073102 (2017).
[16] M. E.Mora-Ramos, F. J. Rodríguez, L. Quiroga, Solid State Communications **109**, 767 (1999).
[17] M. E. Mora-Ramos, F. J. Rodríguez, L. Quiroga, Journal of Physics: Condensed Matter **11**, 8223 (1999).
[18] M. E. Mora-Ramos, L. M. Gaggero-Sager, Physica Status Solidi B **220**, 175 (2000).
[19] M. E. Mora-Ramos, F. J. Rodríguez, L. Quiroga, Physica Status Solidi B **220**, 111 (2000).
[20] R. Salgado-García, M. E. Mora-Ramos, L. M. Gaggero-Sager, Physica Status Solidi B **232**, 138 (2002).
[21] M. Toledo-Solano, M. E. Mora-Ramos, Physica E **19**, 356 (2003).
[22] B. C .Lee, K. W. Kim, M. A. Stroscio, M. Dutta, Physical Review B **58,** 4860 (1998).
[23] J. J. Shi, Physical Review B **68,** 165335 (2003).
[24] L. Li, D. Liu, J. J. Shi, The European Physical Journal B **44,** 401 (2005).
[25] G.. H.Wang, Optik **125,** 2374 (2014).
[26] E. C. Niculescu, N. Eseanu, A. Radu, Optics Communications **294,** 276 (2013).
[27] H. Hassanabadi, G. H Liu, L. L. Lu, Solid State Communications **152,** 1761 (2012).
[28] A. Keshavarz, M. J. Karimi, Physics Letters A **374,** 2675 (2010).
[29] Ozturk Emine, Optik **139,** 256 (2017).
[30] N. T.Tien, N. N. T. Hung, T. T. Nguyen, P. T. B.Thao, Physica B **519,** 63 (2017).
[31] J. H.Yuan, N. Chen, Y. Zhang, H. Mo, Z. H. Zhang, Physica E **77,** 102 (2016).
[32] L. Zhang, Optical and Quantum Electronics **36,** 6 65 (2004).
[33] F. Ungan, J. C. Martínez-Orozco, R. L. Restrepo, M. E. Mora-Ramos, E. Kasapoglu, C. A. Duque, Superlattices and Microstructures **81,** 26 (2015).
[34] F. Ungan, M. E. Mora-Ramos, C. A. Duque, E. Kasapoglu, H. Sari, I. Sökmen, Superlattices and Microstructures **66,** 129 (2014).
[35] E. B.Al, F. Ungan, U. Yesilgul, E. Kasapoglu, H. Sari, I. Sökmen, Optical Materials **47,** 1 (2015).
[36] E. Ozturk, I. Sokmen, Journal of Luminescence **145,** 387 (2014).
[37] M. J. Karimi, A. Keshavarz, Superlattices and Microstructures **50,** 572 (2011).
[38] F. Ungan, U. Yesilgul, E. Kasapoglu, H. Sari, I. Sökmen, Journal of Luminescence **132**, 1627 (2012).
[39] U.Yesilgul, Journal of Luminescence **132**, 765 (2012).
[40] U. Yesilgul, F. Ungan, E. Kasapoglu, H. Sari, I. Sökmen, Physica B **475**, 110 (2015).
[41] B. Chen, K. X. Guo, R. Z. Wang, Z. H. Zhang, Z. L. Liu, Solid State Communications **149**, 310 (2009).
[42] C. J. Zhang, K. X. Guo, Physica B **387**, 276 (2007).

[43] X. X. Liang, X. Wang, Physical Review B **43**, 5155 (1991).
[44] F. Q.Zhao, X. X. Liang, S. L. Ban, International Journal of Modern Physics B **15**, 527 (2001).
[45] F. Q. Zhao, X. X. Liang, Chinese Physics Letters **19**, 974 (2002).
[46] F. Q.Zhao, X. X. Liang, S. L. Ban, The European Physical Journal B **33**, 3 (2003).
[47] F. Q.Zhao, J. Gong, Chinese Physics Letters **24**, 1327 (2007).
[48] S. H. Ha, S. L. Ban, Journal Physics: Condensed Matter **20**, 085218 (2008).
[49] S.Adachi, Journal of Applied Physics **58**, R1 (1985).
[50] D. Z. Y.Ting, Y. C. Chang, Physical Review B **36**, 4359 (1987).
[51] J. M. Wagner, F. Bechstedt, Physical Review B **62**, 4526 (2000).
[52] A. R.Goni, K. Syassen, M. Cardona, Physical Review B **41**, 10104 (1990).
[53] N. Eseanu, Physics Letters A **374**, 1278 (2010).
[54] F.Yun, M. A. Reshchikov, L. He, T. King, H. Morkoc, Journal of Applied Physics **92**, 4837 (2002).
[55] W. R. L.Lambrecht, K. Kim, S. N. Rashkeev, B. Segall, Mater. Res. Soc. Symp. Proc. **395**, 455 (1996).
[56] P. Perlin, I. Gorczyca, N. E. Christensen, I. Grzegorg, H. Teisseyre, T. Suski, Physical Review B **45**, 13307 (1992).
[57] T. Azuhata, T. Sota, K. Suzuki, S. Nakamura, Journal Physics: Condensed Matter **7**, L129 (1995).
[58] J. M.Wagner, F. Bechstedt, Physical Review B **66**, 115202 (2002).
[59] H. Wang, G. A. Farias, V. N. Freire, Physical Review B **60**, 5705 (1999).
[60] S. H.Wei, A.Zunger, Physical Review B **60**, 5404 (1991).
[61] I. Vurgaftman, J, R. Meyer, Journal of Applied Physics **94**, 3675 (2003).
[62] P. Perlin, A. Polian, T. Suski, Physical Review B **47**, 2874 (1993).
[63] F. T. Liu, S. H. Zhang, C. H. Gao, Journal of Shandong Univercity **45**, 69 (2010).
[64] F. Q.Zhao, Z. Z. Guo, International Journal of Modern Physics B **18**, 2991 (2004).

* Corresponding author: zhaofengqi@126.com
phzzguo@126.com